

x liquid-phase concentration, mole fraction
 y vapor-phase concentration, mole fraction

Greek Letters

γ_i activity coefficient
 Π total pressure, mmHg
 Φ ratio of fugacity coefficients
 $\hat{\phi}_i$ fugacity coefficient in vapor mixture at Π
 ϕ_i fugacity coefficient of pure component at P^0

Registry No. Trimethyl borate, 121-43-7; heptane, 142-82-5.

Literature Cited

- (1) Hala, E.; Pick, J.; Friedl, V.; Vllim, O. "Vapor-Liquid Equilibrium", 2nd English ed.; Pergamon Press: Oxford, 1967; pp 305-6.

- (2) Christopher, P. M.; Washington, H. W. *J. Chem. Eng. Data* 1969, 14, 437.
 (3) Munster, N.; Plank, C. A.; Laukhuf, W. L. S.; Christopher, P. M. *J. Chem. Eng. Data* 1984, 29, 178.
 (4) Lange, N. A. "Handbook of Chemistry", 11th ed.; Handbook Publishing: Sandusky, OH, 1973.
 (5) "High Purity Solvent Guide"; Physical Property Section, Burdick and Jackson Laboratories, Inc.: Muskegon, MI, 1980.
 (6) Plank, C. A.; Christopher, P. M. *J. Chem. Eng. Data* 1976, 21, 211.
 (7) Reid, R. C.; Prausnitz, J. M.; Sherwood, T. K. "The Properties of Gases and Liquids", 3rd ed.; McGraw-Hill: New York, 1977; p 432.
 (8) Fredenslund, A.; Gmehling, J.; Rasmussen, P. "Vapor-Liquid Equilibria Using UNIFAC"; Elsevier: Amsterdam, 1977.
 (9) Smith, J. M.; Van Ness, H. C. "Introduction to Chemical Engineering Thermodynamics", 3rd ed.; McGraw-Hill: New York, 1975.

Received for review May 9, 1984. Accepted August 27, 1984.

Sound Velocity and Electrolytic Conductivity in the Molten Sodium Nitrite-Potassium Nitrate System

Shinya Okuyama, Katsusaburo Toyoda,[†] Ryuzo Takagi, and Kazutaka Kawamura*

Research Laboratory for Nuclear Reactors, Tokyo Institute of Technology, Meguro-ku, Tokyo 152, Japan

Sound velocity and electrolytic conductivity in binary molten salt mixtures of NaNO_2 - KNO_3 , which is a candidate for heat reservoir material, were determined by an ultrasonic pulse-echo method and a direct current (dc) method, respectively. The adiabatic and isothermal compressibilities, the isochoric specific heat, and the molar conductivity were derived with available data on isobaric specific heat and density. The concentration dependences of these properties show significant deviation from linearity.

Introduction

Mixtures of NaNO_2 and KNO_3 have as low a melting point as HTS (heat transfer salt; NaNO_2 - KNO_3 - NaNO_3 49/44/7 mol %) and are therefore promising candidates as heat reservoir materials (1). It is useful to know the concentration dependence of properties of the mixture, since a concentration distribution appears in a phenomenon with mass transfer, e.g., corrosion. In this work the sound velocity and the electrolytic conductivity in this mixture have been measured. The sound velocity was measured by an ultrasonic pulse-echo method. The sound velocity gives us some thermodynamic properties, such as adiabatic and isothermal compressibilities, and isochoric specific heat with available data on density and isobaric specific heat. The molar conductivity is derived from the electrolytic conductivity, which was measured by a dc method, and available density data. A dc method in contrast to an ac method produces no polarization impedance (2).

The sound velocity (3) and the electrolytic conductivity (4) of HTS were reported previously. They will be compared with the corresponding quantities obtained in this work.

Experimental Section

Chemicals. The salts NaNO_2 and KNO_3 used were of analytical reagent grade (Wako Chemicals). They were melted and then dispersed with N_2 gas. Additionally they were passed through a glass filter just before experimental run. The content

Table I. Sound Velocity in Molten NaNO_2 - KNO_3 System

$$U \text{ (m s}^{-1}\text{)} = a + bT + cT^2$$

run no.	$P_{\text{NaNO}_2}^a$	$10^{-3}a$	b	10^3c	temp range/K
1	1.000	3.0631	-2.8395	1.3679	571-689
2	0.811	3.2057	-3.3968	1.8228	511-666
3	0.653	2.7257	-1.7523	0.3649	437-649
4	0.491	2.7572	-1.9526	0.5597	444-686
5	0.317	2.9514	-2.6471	1.1114	483-700
6	0.182	3.4120	-3.9913	2.0897	546-681
7	0.000	2.4910	-1.1262	-0.1153	617-747
ref	salts	$10^{-3}a$	b	10^3c	temp range/K
3	NaNO_2	2.7061	-1.470		565-586
3	KNO_3	2.4807	-1.187		625-713
7	KNO_3	2.483	-1.194		593-803
8	KNO_3	2.450	-1.12		609-712
9	KNO_3	2.7663	-1.9149	0.4686	b

^a Mole fraction of NaNO_2 . ^b Unspecified in the literature.

of NaNO_2 , which is reported to be thermally unstable at higher temperatures, was checked before and after each run. The experimental data were accepted when the following relation was satisfied within experimental error:

$$N_{\text{Na}}M_{\text{NaNO}_2} + N_{\text{K}}M_{\text{KNO}_3} = W \quad (1)$$

In eq 1 W is the weight of the mixture sampled from the melt, N_X is the molar quantity of a component cation X , and M_Y is the formula weight of a component salt Y . The quantities N_{Na} and N_{K} were determined by flame spectrophotometry. Relative error in N_{Na} and N_{K} was estimated to be $\pm 2\%$. During each experimental run the sample melts were kept under N_2 gas atmosphere to depress the decomposition of NaNO_2 (5).

Sound Velocity Experiment. Figure 1 shows a schematic diagram of the apparatus, which is equipped with three micrometers (b). Except for this modification the apparatus is similar to that employed previously (3). These micrometers are used to adjust parallelism between planes of the quartz conductivity rod (f) and the bottom of the cell (j). The experimental procedure was described in detail previously (3).

Electrolytic Conductivity Experiment. The experimental equipment and technique are similar to those used by King and Duke (6). The cell constant was 14.90 cm^{-1} , which was de-

[†] Shibaura Institute of Technology, Shibaura, Minato-ku, Tokyo 108, Japan.

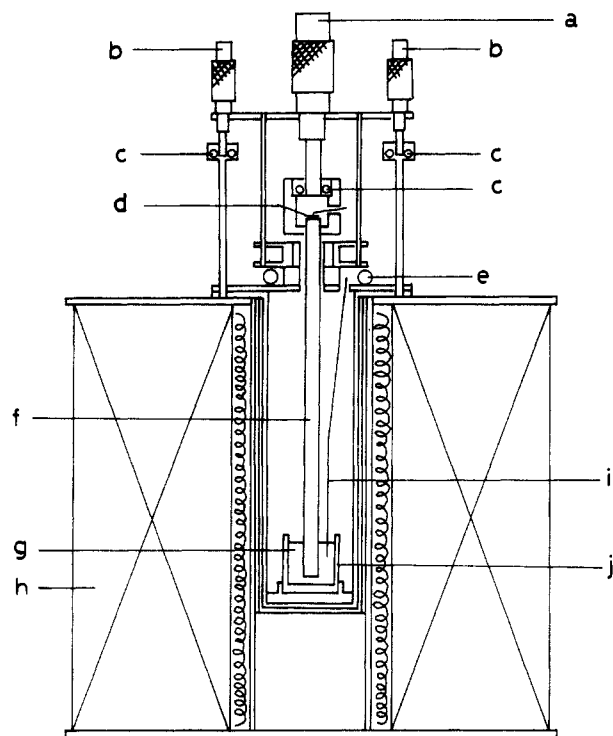


Figure 1. Schematic diagram of the apparatus used for an ultrasonic pulse-echo method: (a) micrometer for measurement of change of sound path length, (b) micrometer for adjustment of parallelism, (c) bearing, (d) X-cut quartz crystal transducer, (e) pipe for water cooling, (f) conductor rod, (g) molten salt, (h) electric furnace, (i) thermocouple, (j) cell.

Table II. Concentration Variation of NaNO_2 Before and After Experimental Runs for Sound Velocity

run no.	P_{NaNO_2}	
	before run	after run
2	0.811	0.811
3	0.654	0.652
4	0.495	0.487
5	0.314	0.320
6	0.183	0.180

terminated by a KCl standard solution.

Results and Discussion

The experimental results for the sound velocity are listed in Table I with other workers' results. The original data on sound velocity are provided as supplementary material (see paragraph at end of text regarding supplementary material). The concentrations of NaNO_2 before and after experimental runs are listed in Table II, which shows that heating the melts containing NaNO_2 up to ~ 700 K brought no significant concentration change under N_2 gas atmosphere within analytical error ($\pm 2\%$). The sound velocity of NaNO_2 reported by Mikami et al. (3) is significantly different from our result. It might be conjectured that the decomposition of NaNO_2 in their experiment brought such a discrepancy.

The adiabatic compressibility (β_s) is related to the sound velocity (U) as follows:

$$\beta_s = 1/\rho U^2 \quad (2)$$

where ρ is the density. The isothermal compressibility (β_T) and the isochoric specific heat (C_V) are obtained from the following relations:

$$\beta_T = \beta_s + TV\alpha^2/C_p \quad (3)$$

$$C_V = C_p\beta_s/\beta_T \quad (4)$$

Table III. Adiabatic Compressibility Estimated According to Eq 2

$$\beta_s (\text{m}^2 \text{N}^{-1}) = a + bT + cT^2$$

P_{NaNO_2}	$10^{10}a$	$10^{13}b$	$10^{16}c$
1.000	0.112	2.376	0.302
0.811	-0.003	2.780	0.025
0.653	0.851	-0.272	2.787
0.491	0.790	-0.010	2.576
0.317	0.526	0.829	1.944
0.182	-0.201	2.900	0.050
0.000	1.808	-3.328	5.247

Table IV. Isothermal Compressibility Estimated According to Eq 3

$$\beta_T (\text{m}^2 \text{N}^{-1}) = a + bT + cT^2$$

P_{NaNO_2}	$10^{10}a$	$10^{13}b$	$10^{16}c$
1.000	0.207	2.211	1.056
0.811	0.069	2.697	0.729
0.653	0.903	-0.279	3.441
0.491	0.852	-0.051	3.279
0.317	0.608	0.724	2.776
0.182	-0.103	2.745	1.346
0.000	1.972	-3.688	6.289

Table V. Isochoric Specific Heat Estimated According to Eq 4

$$C_V (\text{J K}^{-1} \text{mol}^{-1}) = a + bT + cT^2$$

P_{NaNO_2}	$10^{-2}a$	10^2b	10^6c
1.000	1.077	-0.756	-0.669
0.811	1.092	-0.505	-0.885
0.653	1.201	-3.603	1.834
0.491	1.224	-3.302	1.493
0.317	1.227	-2.175	0.551
0.182	1.174	0.2766	-1.298
0.000	1.406	-5.444	2.972

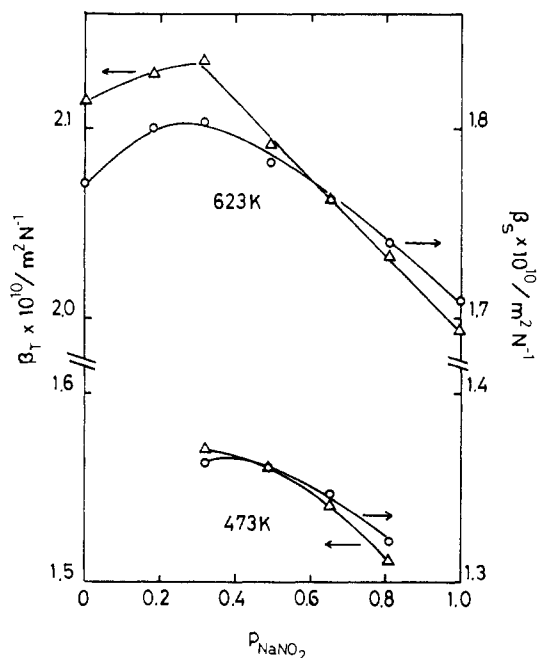


Figure 2. Isotherms of adiabatic and isothermal compressibilities in molten NaNO_2 - KNO_3 system.

where T , V , α , and C_p are temperature, molar volume, thermal expansivity, and isobaric specific heat, respectively. The isothermal compressibility of KNO_3 at 623 K was estimated to be $2.34 \times 10^{-10} \text{ m}^2 \text{N}^{-1}$, which satisfactorily agrees with $2.25 \times 10^{-10} \text{ m}^2 \text{N}^{-1}$ as determined by p - V - T measurement (10). As for the molten NaNO_2 - KNO_3 system, its adiabatic and isother-

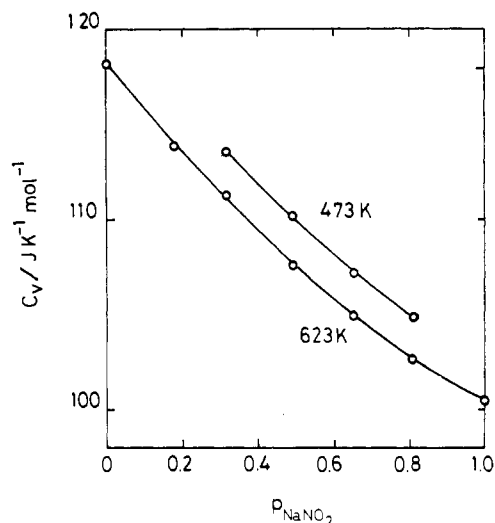


Figure 3. Isotherms of isochoric specific heat in molten $\text{NaNO}_2\text{-KNO}_3$ system.

Table VI. Electrolytic and Molar Conductivity of Pure Melts NaNO_2 and KNO_3

T/K	$10^{-2}\kappa/(\text{S m}^{-1})$	$10^3\Lambda/(\text{S m}^2 \text{mol}^{-1})$	$10^{-2}\kappa^b/(\text{S m}^{-1})$
NaNO_2			
609	1.549	6.05 ^a	1.538 ^d
610	1.559	6.09 ^a	1.543 ^d
637	1.705	6.73 ^a	1.690 ^d
641	1.723	6.81 ^a	1.712 ^d
643	1.730	6.85 ^a	1.723 ^d
664	1.855	7.40 ^a	1.838 ^d
666	1.852	7.39 ^a	1.849 ^d
673	1.890	7.56 ^a	1.887 ^d
KNO_3			
626	0.658	3.59, ^a 3.65 ^c	0.675, ^e 0.669 ^f
641	0.713	3.91, ^a 3.93 ^c	0.724, ^e 0.717 ^f
653	0.758	4.18, ^a 4.15 ^c	0.762, ^e 0.754 ^f
668	0.804	4.46, ^a 4.43 ^c	0.808, ^e 0.800 ^f
681	0.844	4.70, ^a 4.68 ^c	0.847, ^e 0.839 ^f
694	0.880	4.93, ^a 4.92 ^c	0.885, ^e 0.877 ^f

^a Estimated with available density (8). ^b Interpolated from reported data. ^c Estimated with the least-squares representation (14). ^d Reference 13. ^e Reference 6. ^f Reference 14.

mal compressibilities, and isochoric specific heat calculated with available data on density (11) and isobaric specific heat (12), are listed in Tables III–V, respectively. Isotherms of these data are shown at 473 and 623 K in Figure 2 and 3.

Results for the electrolytic conductivity are listed in Table VI for pure melts NaNO_2 and KNO_3 with other workers' results, and in Table VII for the molten $\text{NaNO}_2\text{-KNO}_3$ system. For the molten KNO_3 , several workers have reported its electrolytic conductivity, which was discussed by Robbins and Braunstein (14). Robbins and Braunstein also determined it carefully by an ac method. As shown in Table VI, our result is comparable with their result. Isotherms of the electrolytic and molar conductivities at 623 K are shown in Figure 4. Figures 2 and 3 shows significant deviation from additivity. The sound velocity (9) and the electrolytic conductivity (6) for the molten $\text{NaNO}_2\text{-KNO}_3$ system are reported. Corresponding quantities in the molten $\text{NaNO}_3\text{-KNO}_3$ system show greater linearity with concentration than those in the molten $\text{NaNO}_2\text{-KNO}_3$ system. Replacement of NO_2 for NO_3 in NaNO_3 seems to introduce some structural change.

The melting point of the $\text{NaNO}_2\text{-KNO}_3$ system reaches a minimum of 416 K at $p_{\text{NaNO}_2} = 0.52$ (15), where p_{NaNO_2} is the mole fraction of NaNO_2 . The sound velocity and the electrolytic conductivity in the molten $\text{NaNO}_2\text{-KNO}_3$ with $p_{\text{NaNO}_2} = 0.52$ are estimated to be 1758 m s^{-1} and 98.0 S m^{-1} at 623 K, re-

Table VII. Electrolytic and Molar Conductivities in Molten $\text{NaNO}_2\text{-KNO}_3$ System

T/K	$10^{-2}\kappa/(\text{S m}^{-1})$	$10^3\Lambda/(\text{S m}^2 \text{mol}^{-1})$	T/K	$10^{-2}\kappa/(\text{S m}^{-1})$	$10^3\Lambda/(\text{S m}^2 \text{mol}^{-1})$
$p_{\text{NaNO}_2} = 0.701$			$p_{\text{NaNO}_2} = 0.378$		
594	1.050	4.55	621	0.855	4.16
615	1.149	5.02	634	0.901	4.41
631	1.216	5.35	650	0.982	4.84
648	1.285	5.69	661	1.019	5.04
660	1.347	5.99	682	1.151	5.73
677	1.426	6.37	686	1.114	5.56
$p_{\text{NaNO}_2} = 0.508$					
589	0.847	3.91			
604	0.907	4.21			
618	0.961	4.49			
640	1.046	4.92			
658	1.111	5.26			
659	1.115	5.28			
684	1.220	5.84			

^a Estimated with available density (8).

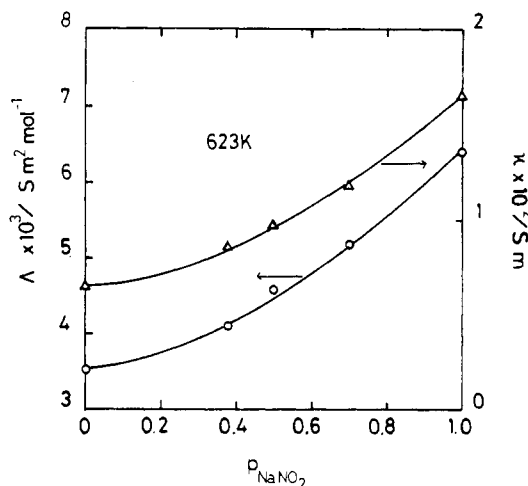


Figure 4. Isotherms of electrolytic and molar conductivities in molten $\text{NaNO}_2\text{-KNO}_3$ system.

spectively, which are comparable with 1765 m s^{-1} (3) and 105.5 S m^{-1} (4) in HTS.

Acknowledgment

The electrolytic conductivity experiment was carried out at Professor Okada's laboratory. We thank Professor Okada for his kindness.

Glossary

a, b, c	constants in empirical equations
C_p	isobaric specific heat, $\text{J K}^{-1} \text{mol}^{-1}$
C_v	isochoric specific heat, $\text{J K}^{-1} \text{mol}^{-1}$
M_Y	formula weight of component salt Y, kg mol^{-1}
N_X	molar quantity of component ion X, mol
p_{NaNO_2}	mole fraction of NaNO_2
T	temperature, K
U	sound velocity, m s^{-1}
V	molar volume, $\text{m}^3 \text{mol}^{-1}$
W	weight, kg

Greek Letters

α	expansivity, K^{-1}
β_s	adiabatic compressibility, $\text{m}^2 \text{N}^{-1}$
β_T	isothermal compressibility, $\text{m}^2 \text{N}^{-1}$
κ	electrolytic conductivity, S m^{-1}
Λ	molar conductivity, $\text{S m}^2 \text{mol}^{-1}$
ρ	density, kg m^{-3}

Registry No. KNO_3 , 7757-79-1; NaNO_2 , 7632-00-0.

Literature Cited

- (1) Kamimoto, M.; Sakuta, K.; Ozawa, T.; Sakamoto, R. *Circ. Electrotech. Lab.* **1978**, No. 196, 10.
- (2) Takagi, R.; Shimotake, H. *New Mater. New Processes* **1983**, 2, 332.
- (3) Mlkami, M.; Odawara, O.; Kawamura, K. *J. Chem. Eng. Data* **1981**, 26, 411.
- (4) Uchiyama, Y.; Kawamura, K. *J. Chem. Eng. Data* **1981**, 26, 407.
- (5) Stern, K. J. *Phys. Chem. Ref. Data* **1972**, 1, 747.
- (6) King, L. A.; Duke, F. R. *J. Electrochem. Soc.* **1964**, 6, 712.
- (7) Bockris, J. O'M.; Richards, N. E. *Proc. R Soc. London, Ser. A* **1957**, 241, 44.
- (8) Higgs, R. W.; Litovitz, T. A. *J. Acoust. Soc. Am.* **1960**, 32, 1108.
- (9) Cerlsier, P.; Finiels, G.; Doucet, Y. *J. Chim. Phys. Phys.-Chim. Biol.* **1974**, 6, 836.
- (10) Bannard, J. E.; Barton, A. F. M. *J. Chem. Soc., Faraday Trans. 1* **1976**, 74, 153.
- (11) Polyakov, V. D.; Berull, S. H. *Izv. Sekt. Fiz.-Khim. Anal., Inst. Obshch. Neorg. Khim., Akad. Nauk SSSR* **1955**, 26, 164.
- (12) Iwadate, Y.; Okada, I.; Kawamura, K. *J. Chem. Eng. Data* **1982**, 27, 288.
- (13) Bloom, H.; Knaggs, I. W.; Molloy, J. J.; Welch, D. *Trans. Faraday Soc.* **1953**, 49, 1458.
- (14) Robbins, G. D.; Braunstein, J. J. *Electrochem. Soc.* **1969**, 116, 1218.
- (15) Berull, A. I.; Bergman, A. G. *Izv. Sekt. Fiz. Khim. A* **1954**, 25, 218.

Received for review May 30, 1984. Accepted October 5, 1984.

Supplementary Material Available: A table of original data on sound velocity in the molten NaNO₂-KNO₃ system (2 pages). Ordering information is given on any current masthead page.

Viscosity and Lithium-7 Nuclear Magnetic Resonance Relaxation Time of Concentrated Lithium Nitrate-Ammonia Solutions

Katsuyuki Uchibayashi, Masahito Niibe, and Yoshio Nakamura*

Department of Chemistry, Faculty of Science, Hokkaido University, 060 Sapporo, Japan

The viscosity coefficient and density of concentrated LiNO₃-NH₃ solutions (up to 30 mol % LiNO₃) have been determined as a function of composition and temperature. The observed viscosity coefficient and its activation energy show a change in composition dependence around 10 mol % LiNO₃. The spin-lattice relaxation time of ⁷Li has also been measured and correlated to the present viscosity data.

Introduction

Lithium nitrate (LiNO₃) is very soluble in liquid ammonia (NH₃); the saturated solution at room temperature contains about 35 mol % LiNO₃. Three compounds, LiNO₃·2NH₃, LiNO₃·4NH₃, and LiNO₃·8NH₃ are known from the study of the phase diagram (1). It will be of great interest to study transport phenomena in such concentrated solutions of an ionic solute in a molecular solvent (2). No data on the viscosity coefficient of the LiNO₃-NH₃ system are available, though the viscosity coefficients of various salt-ammonia systems have been reported by Kikuchi (3) many years ago. The purpose of the present study was to determine the viscosity coefficient of the LiNO₃-NH₃ system as a function of composition and temperature. The density of this system has also been measured in order to check the existing data (4). Measurements have also been made on the spin-lattice relaxation time of ⁷Li in the present system, which is correlated to the results of the viscosity measurements. The present data will serve for better understanding of the transport properties of concentrated electrolyte solutions in polar solvents.

Experimental Section

Material. NH₃ (99.99%, Seitetsu Kagaku Co.) passed through a column with pellets of NaOH was liquefied and treated with lithium metal to remove trace of water and oxygen. It was then distilled over pieces of sodium metal several times and stored in a vessel as a saturated solution of LiNO₃. Reagent-grade LiNO₃ (Wako Pure Chemical Ltd.) was dried at 110 °C over 24 h and used without further purification. Sample solutions were prepared by distilling purified NH₃ into each measuring cell containing a desired amount of LiNO₃ dried under vacuum. The composition of each sample solution was cal-

culated from the weight of the components.

Apparatus and Procedures. The viscosity coefficient of sample solutions was determined with a sealed Ubbelohde type viscometer. The viscometer is about 20 cm in height and has a capillary part of about 8 cm in length, which was immersed in an alcohol bath controlled within ±0.03 °C. The viscosity coefficient η by using the relation

$$\eta = C_1 \rho t - C_2 \rho / t \quad (1)$$

The constants C_1 and C_2 for each viscometer were determined by using pure methanol with the known values of the viscosity coefficient and density (5). The density of sample solutions was determined for some representative compositions by use of a sealed dilatometer whose volume was about 5 cm³. Estimated errors in ρ , t , and η in the present measurements were ±0.3%, ±0.5%, and ±1%, respectively.

NMR measurements were made with a Bruker SXP 4-100 spectrometer operating at 34.98 MHz for ⁷Li. Each sample solution was put into a measuring cell of 8-mm inner diameter. The spin-lattice relaxation time T_1 was measured by using the standard 180°- τ -90° pulse sequence method. Temperatures of samples were controlled within 1 °C by a stream of cooled nitrogen gas.

Results and Discussion

The results for the density, ρ , of the LiNO₃-NH₃ system at 20 °C are expressed as

$$\rho(20\text{ }^\circ\text{C}) = 0.6150 + 2.625X - 2.400X^2 \text{ (g/cm}^3\text{)} \quad (2)$$

where X is the mole fraction of the solute (LiNO₃). The present results are in good agreement with those given in the literature (4). The results at -50 °C are also given by

$$\rho(-50\text{ }^\circ\text{C}) = 0.7076 + 2.151X - 1.330X^2 \text{ (g/cm}^3\text{)} \quad (3)$$

On the other hand, the experimental results for the viscosity coefficient, η , can be expressed by the Andrade equation

$$\log \eta = A/T + B \quad (4)$$

as a function of the absolute temperature T . The experimental values of the constants A and B for each sample solution are